Sensors & Diagnostics

PAPER

View Article Online
View Journal

Cite this: DOI: 10.1039/d6sd00034g

Establishment of a peptide-based electrochemical immunosensor for detecting antibodies against the GP5 protein from the porcine reproductive and respiratory syndrome virus

Luis Enrique Franco-Correa, [a] Luis A. Ortiz-Frade, [b] Alejandro Bravo Patiño, [a] Francisco Perez-Duran, [a] Fernando Calderón-Rico, [a] Alicia Gabriela Zamora-Avilés, [a] Martha Leticia Jiménez-González, [b] Gabriel Espinosa, [c] Daniel Durand-Herrera, [a] Ricarda Cortés-Vieyra [a] and Rosa Elvira Nuñez-Anita *[a]

Porcine reproductive and respiratory syndrome (PRRS) is one of the most economically devastating diseases that affect the swine industry worldwide. Although enzyme-linked immunosorbent assays (ELISAs) are the gold standard for analyzing antibodies against viruses, they have some limitations, such as sample transport and analysis times and cost. Rapid serological surveillance of PRRSV remains a critical challenge for swine health management. Immunosensors are feasible diagnostic alternatives, where antigen–antibody interactions can be immediately quantitatively determined. Electrochemical sensor operation is based on changes in interfacial electron transfer at the working electrode surface, which are monitored using electrochemical impedance spectroscopy (EIS). In this approach, a redox probe ($[Fe(CN)_6]^{3-}/[Fe(CN)_6]^{4-}$) is used to evaluate the charge-transfer resistance (R_{ct}) at the electrode interface. Variations in analyte concentration lead to changes in the interfacial properties of the electrode, particularly after biomolecular interactions such as antibody binding. These interactions hinder electron transfer, resulting in an increase in R_{ct}. The analytical signal is therefore based on the correlation between the change in R_{ct} (ΔR_{ct}) and the concentration of the target analyte, enabling quantitative analysis through calibration plots. The goal was the establishment of a peptide based electrochemical immunosensor for quantifying antibodies against PRRSV. Gold electrode functionalization was characterized using EIS, the GP5-B peptide, and casein protein. Balb/c mice were immunized according to control, BSA-immunized, and GP5-B peptide-immunized groups. Control pigs were free from the porcine respiratory disease complex (PRDC) and nonvaccinated. Vaccinated pigs were injected using commercial Ingelvac vaccine according to the manufacturer's instructions, and naturally infected pigs were also included in the study. Antibodies were measured using ELISA assays and an immunosensor. The immunosensor recognized antigen–antibody interactions, with a limit of detection (LOD) of 6 ng mL^{-1}, a repeatability of intra-assay CV of 5.05%, and a reproducibility inter-assay CV of 4.08% through batch to batch. Additionally, it achieved a sensitivity of 100%, and a specificity of at least 93%. Considering all the data, compared to immunoglobulin G detection *via* ELISAs, the proposed peptide-based electrochemical immunosensor is valuable for detecting antibodies against PRRSV. These results suggest the feasibility of biosensors for serological diagnosis in pigs.

Received 12th February 2026,
Accepted 19th April 2026

DOI: 10.1039/d6sd00034g

rsc.li/sensors

[a] *Facultad de Medicina Veterinaria y Zootecnia, Posta Veterinaria y Zootecnia de la Universidad Michoacana de San Nicolás de Hidalgo, Universidad Michoacana de San Nicolás de Hidalgo, Edificio G. Km. 9.5 S/N, Carretera Morelia-Zinapécuaro, C.P. 58893, La Palma, Tarímbaro, Michoacán, Mexico.*
E-mail: rosa.anita@umich.mx; Fax: +52 (443) 295 8029; Tel: +52 (443) 295 8029
[b] *Centro de Investigación y Desarrollo Tecnológico en Electroquímica S.C., Parque Tecnológico Querétaro S/N, 76700 Santiago de Querétaro, Querétaro, Mexico*
[c] *Instituto de Física y Matemáticas, Universidad Michoacana de San Nicolás de Hidalgo, Francisco J. Mújica S/N, Ciudad Universitaria, 58070 Morelia, Michoacán, Mexico*

Introduction

Porcine reproductive and respiratory syndrome (PRRS) remains one of the most economically devastating infectious diseases affecting the global swine industry. It is characterized by severe reproductive failure in pregnant sows and persistent respiratory distress in pigs of all ages, frequently resulting in significant production losses and

increased mortality rates.[1,2] In some cases, outbreaks have been associated with vaccine-derived virus strains, further complicating disease control and herd management.[3,4] The etiological agent, porcine reproductive and respiratory syndrome virus (PRRSV), is an enveloped virus approximately 45–80 nm in diameter with an asymmetric capsid and a positive-sense single-stranded RNA genome of approximately 15 Kb. PRRSV belongs to the genus *Porarterivirus*, within the family *Arteriviridae*.[5,6] The viral genome comprises at least 11 open reading frames (ORFSs), among which the structural glycoprotein GP5, encoded by ORF5, represents one of the most immunogenic viral proteins. GP5 contains key B-cell epitopes that induce the production of neutralizing antibodies,[7,8] making it a critical target for serological diagnosis and vaccine development. Consequently, GP5-based approaches are highly relevant for both PRRSV diagnosis and epidemiological surveillance.[8]

PRRSV infection is commonly detected either directly by polymerase chain reaction (PCR)-based molecular assays or indirectly through serological techniques such as enzyme-linked immunosorbent assay (ELISAs). Although these methods are widely used, they often require specialized laboratory infrastructure, trained personnel, complex sample handling procedures, and long processing times, which may limit their applicability under field conditions.[9,10] Despite advances in serological diagnostics, rapid, cost-effective point-of-care methods for PRRSV antibody detection remain limited.[9]

Electrochemical immunosensors have emerged as promising alternatives for pathogen detection due to their high sensitivity, relatively low cost, rapid response times, and compatibility with miniaturized and portable analytical devices.[11] These characteristics make them particularly attractive for point-of-care testing (POCT) in veterinary diagnostics and livestock health monitoring.[12,13] Several electrochemical immunosensing strategies have been reported for viral detection.

For example, a gold immunochromatographic strip coupled with an electrochemical reader was used to quantify anti-Newcastle disease virus; other systems include a label-free sensor for infectious bursal disease virus (IBDV) with a limit of detection (LOD) of ~14 particles per mL,[14] and impedance-based platforms for avian influenza A (H5N1).[15] In swine diagnostics, sensors have been implemented for H1N1 influenza,[16] porcine circovirus 2 (PCV2),[17] and pseudorabies virus (PRV) using magnetic beads to achieve a wide linear range.[18]

In recent years, peptide-based biosensors have attracted increasing attention as alternative to whole-protein recognition elements.[13] Synthetic peptides offer several advantages, including high chemical stability, reproducible synthesis and lower production cost.[19,20] Their relatively small size facilitates controlled immobilization on electrode surfaces and promotes well-defined molecular orientation, which can enhance electron transfer efficiency and improve sensor performance.[13,21] We hypothesized that a synthetic peptide derived from the GP5 protein could serve as a stable and selective recognition element for electrochemical detection of anti-PRRSV antibodies, enabling rapid serodiagnosis compared with conventional immunoassays.

In this context, we comparatively evaluated the analytical performance of the GP5-derived synthetic peptide using both conventional ELISA and an electrochemical impedimetric immunosensor platform. The proposed sensor integrates a peptide-based recognition interface with a self-assembled monolayer-modified gold electrode to enable label-free detection of anti-PRRSV antibodies. This approach addresses the growing demand for rapid, portable, and cost-effective serological tools for veterinary disease surveillance. These electrochemical platforms may contribute to improved biosecurity strategies, rapid outbreak monitoring, and enhanced animal health management in the swine industry.[22]

To our knowledge, this is the first electrochemical immunosensor based on a GP5-derived peptide for PRRSV antibody detection, tested in both experimental murine immunization and vaccinated/naturally infected swine.

Materials and methods

Peptide

A peptide derived from the GP5 sequence of PRRSV type 2 (GP5-B)[7] was chemically synthesized by GenScript (La Joya, USA). The GP5-B sequence comprised ASNDSSSHLQLIYNLTLCELNGTDWLANKF (30 amino acids; around approximately 3.3–3.4 kDa), and the peptide was 95% pure and soluble in dimethyl sulfoxide (DMSO).

Mouse immunization

Eighteen 7 week-old male mice (Balb/C; Harlan, Indianapolis, IN) were randomly separated into three groups, each comprising six animals, as follows: intact (control mice), albumin control (bovine serum albumin (BSA)-immunized), and GP5-B-immunized (GP5-B peptide binding to BSA) groups. The mice were immunized subcutaneously. For the control and BSA groups, a total volume of 120 μL was administered to each animal; the mixture comprised 30 μL of 1 mg mL^{-1} BSA–maleimide (Imject™ maleimide-activated BSA, Thermo Fisher), 30 μL of DMSO (vehicle), and 60 μL of Freund's complete adjuvant (Sigma-Aldrich), substituting incomplete Freund's adjuvant for the complete adjuvant in booster immunizations.

For the GP5-B-immunized group, a volume of 120 μL was administered to each animal; the mixture comprised 30 μL of 1 mg mL^{-1} GP5-B and 30 μL of 1 mg mL^{-1} maleimide (Imject™ maleimide-activated BSA, Thermo Fisher), conjugated according to the manufacturer's specifications, and 60 μL of complete Freund's adjuvant (Sigma-Aldrich), substituting incomplete Freund's adjuvant for the complete adjuvant in booster immunizations.

The mice were subcutaneously injected using an immobilizer and without anesthesia and were kept in a

temperature-controlled environment at 22 °C ± 1 °C and 50% relative humidity in addition to a 12 : 12 h light–dark cycle. The mice were fed Purina-certified rodent chow and water on demand, and their body weights were recorded every 3 d. The procedures were approved by the local ethics committee, CICUMSNH-A103-FMVZ.

Blood samples were drawn from the immunized mice by puncturing the tail vein using 0.80 mm diameter needles, while the mice were confined using an immobilizer. Blood was collected using Pasteur pipettes moistened with 60 mM ethylenediaminetetraacetate (EDTA) at pH 8. Blood samples were centrifuged at 2500 rpm for 5 min to obtain serum, which was stored frozen at −20 °C. For immunization, the mice were held down by the skin of the back and tail for subcutaneous injection. The mice were followed up over time, with blood samples drawn 45 days after immunization.

Swine serum samples

Serum sampling from control pigs and pigs immunized using a commercial vaccine. Serum samples were obtained from piglets, as originally described in our previous study.[7,23] Briefly, piglets (large white × Piétrain crossbreed, 21 days old, weaned, and mixed sex) were procured from a certified farm (El Dapo Farm, Michoacán, Mexico), which operates under Good Livestock Practices in accordance with the Mexican Official Norm NOM-033-ZOO-199, as previously reported.[7,23]

Serum samples from an immunosensor activity assay were collected at 42 days post immunization (dpi) *via* jugular venipuncture from a group of piglets that received a single intramuscular dose of Ingelvac–PRRSV, MLV® (2 mL containing a 50% tissue culture infectious dose ($TCID_{50}$) of $10^{4.9}$ PRRSV at day 0), and negative control sera were obtained from age-matched, nonimmunized piglets (n = 6 per group); all the animals were housed and allocated under the previously approved protocol CICUMSNH-A101-FMVZ, following the previously described method.[7]

The piglets were housed following approved animal welfare protocols and randomly allocated into treatment groups using the GraphPad random number generator. For this work, serum samples were specifically collected from the group intramuscularly immunized using the commercial vaccine Ingelvac PRRS MLV (Boehringer Ingelheim). The piglets received a single 2 mL intramuscular dose (containing live attenuated PRRSV strain ATCC VR-2332, as specified by the manufacturer) at day 0. Serum was collected at 42 dpi *via* jugular venipuncture. Negative control sera were obtained from age-matched, nonimmunized piglets maintained under the same housing and management conditions (n = 6 per group).

Serum sampling from PRRSV-infected pigs. Serum samples were obtained from an independent group of pigs, as previously described.[23] Serum samples from naturally infected, nonvaccinated pigs (n = 6) were donated by El Limón Farm (Tarimbaro, Michoacán, Mexico) during 2022, at the grower stage of development.[23] Previous data showed the presence of other coinfections associated with the porcine respiratory complex, such as porcine circovirus type 2 (PCV-2), swine influenza virus (H1N1), and *Mycoplasma hyopneumoniae*.[23]

Live subject statements

All animal procedures were performed in accordance with the Guidelines for Care and Use of Laboratory Animals of Norma official Mexicana NOM-062-ZOO-1999 (technical specifications for the production, care, and use of laboratory animals, mice and pigs). The procedures were approved by the Institutional Animal Care and Use of the Faculty of Veterinary Medicine and Zootechnics of the Universidad Michoacana de San Nicolás de Hidalgo (UMSNH), CICUMSNH-A103-FMVZ. Pigs' sera were from cryopreserved samples, previously approved as described.[7,23]

ELISA antibody detection

Peptide-specific antibodies were indirectly quantified using ELISA and a commercial peptide-coating kit (Takara, Shiga, Japan). Following the manufacturer's instructions and the previously described method,[7] 96-well plates were coated with 4 μg mL^{-1} of each GP5-B peptide. Serum samples of 1 μL from immunized mice were tested, and the peptide-specific antibody data are reported in nanograms per milliliter, according to the IgG calibration curve, as previously described.[5]

Preparation of the self-assembled monolayer (SAM)

The formation of the SAM on gold-coated screen-printed electrodes (AuSPEs) was monitored using EIS under the following conditions: EIS data were obtained at a 0.01 V amplitude perturbation from 10 mHz to 100 kHz. The potential was established using the redox couple $[Fe(CN)_6]^{3-}/[Fe(CN)_6]^{4-}$. All the measurements were performed using 5 mM $[Fe(CN)_6]^{4-}/[Fe(CN)_6]^{3-}$ in phosphate-buffered saline (PBS) at pH 7.2. The data obtained were analyzed using EC-Lab (data analysis and processes) and ZView® software (Scribner Associates Inc., Southern Pines, North Carolina).

Prior to self-assembling monolayers, the electrodes were washed with ethanol and distilled water. Initially, the working electrode was modified by adding 10 μL of a 50 mM thioglycolic acid (TGA) solution in ethanol, drying the electrode at room temperature, adding another 10 μL of the TGA solution, and redrying the electrode. The entire process required approximately 15 min. Then, the electrodes were washed with distilled water. The electrode was exposed twice to the thioglycolic acid (TGA) solution with an intermediate drying step to promote controlled and reproducible self-assembled monolayer formation on the gold surface. This stepwise deposition protocol was empirically optimized and monitored by electrochemical impedance spectroscopy (EIS).

For activating the –COOH groups of the formed SAM, 0.4 M *N*-hydroxysuccinimide (NHS) and 0.1 M 1-ethyl-3-(3-dimethylaminopropyl)carbodiimide (EDC) were mixed with

ethanol in a 1 : 1 ratio, and 10 μL of the mixture was added to the working electrode and allowed to react for 30 min to self-assemble the monolayer. Then, the electrode was washed with ethanol and stored in PBS at pH 7.2 until use within 5 h.

For peptide immobilization, NHS was also used to prepare amine-reactive esters of carboxylate groups. Carboxylates (–COOH) were reacted with NHS in EDC, producing esters, which could then react with primary amines ($–NH_2$), forming amide crosslinks. Although NHS is not required for EDC reactions, it substantially improves the coupling efficiency. Both NHS and EDC are soluble in aqueous and organic solvents. However, NHS activation decreases the water solubility of the modified carboxylate molecule so that it dissolves in ethanol. Additionally, because NHS esters have a half-life of 4–5 h at pH 7.2, the peptides were immobilized in this step.

GP5-B peptide immobilization on the SAM-modified electrode

For recognizing the anti-GP5-B antibody, the GP5-B peptide was incorporated into the SAM-modified electrode TGA/NHS/EDC. The SPE was washed using PBS, and excess PBS was removed. Then, 20 μL of the peptide dissolved in PBS (at 50 μg mL^{-1}) was placed on each working electrode and allowed to react for 1 h at room temperature. Finally, the electrodes were rewashed using PBS and stored in PBS at 4 °C until use.

Blockage of nonspecific unions

After the peptide was immobilized on the electrode surface, the biosensor's nonspecific binding sites were blocked. The electrodes were removed from the storage buffer, excess liquid was removed, and the electrodes were incubated with 50 μL of a blocking solution comprising 0.03% casein dissolved in PBS at pH 7.2 and allowed to react for 30 min at room temperature. The binding efficiency was checked using EIS, and the biosensors were rewashed with PBS and refrigerated in PBS at pH 7.2 until use. All the steps of the immunosensor's formation were monitored using EIS.

Electrochemical measurements

The AuSPEs were placed in the electrode holder slot of a cell containing a conical well. The cell was closed, and the conical well was filled with reading solution. The output connector of the AuSPEs was connected to the adapter cable of a potentiostat. EIS measurements were performed at a sinusoidal perturbation of 10 mV over a frequency range from 10 mHz to 100 kHz, using the redox couple $[Fe(CN)_6]^{3-}$/$[Fe(CN)_6]^{4-}$ in PBS (pH 7.2). The measurements were carried out at the open circuit potential (OCP) of the system. This potential corresponds to the equilibrium condition of the redox probe, minimizing polarization effects and ensuring that the measured impedance reflects interfacial properties rather than faradaic processes driven by applied overpotential. Under these conditions, variations in charge-transfer resistance (R_{ct}) can be directly associated with surface modifications and biomolecular interactions occurring at the electrode interface. Subsequently, the data obtained were analyzed using EC-Lab (data analysis and processes) and ZView® (Scribner Associates Inc., Southern Pines, North Carolina).

Peptide–antibody interactions measured using the biosensors

The biosensors were exposed to serum samples prior to a calibration reading without a sample. From the different experimental groups, 1 μL of the serum was added to each sample, mixed with 19 μL PBS dilution buffer to maximize contact with biosensor surfaces, and then incubated with the biosensors for 30 min at room temperature. Then, the electrodes were washed with PBS, and the immunosensors were introduced to the measurement cell for analysis using EIS.

Peptide–antibody interactions measured using ELISA assays

Anti-GP5-B-peptide IgG antibodies were quantified using a peptide-coating kit (Takara, catalog No. MK100) according to the manufacturer's instructions. Briefly, 1 μL of the serum was added to each sample and was mixed with 99 μL dilution buffer, and the reading was recorded using an ELISA plate microplate reader (BIO-RAD iMARK).

Statistical analysis

The data show the results of at least four independent triplicate experiments. The differences between the experimental groups were analyzed using one-way analysis of variance (one-way ANOVA) followed by Tukey's *post hoc* test. Differences of $p \leq 0.05$ were considered as statistically significant. For analyte addition, linear regression was performed. The antibody sensitivity and specificity were calculated using the formulas TP/(TP + FN) and TN/(FP + TN), respectively, and analyzed using Prism (version 9.1.1, GraphPad Software, San Diego, USA) and a receiver operating characteristic (ROC) curve, and the results are shown in Table 1.

Results

We previously reported the immunogenicity of the synthetic GP5-B peptide, derived from the PRRSV GP5 envelope protein, in pigs.[7] In order to compare, mice were immunized

Table 1 Antibody sensitivity and specificity

Anti-PRRSV antibodies			
		+	–
Test	+	**True positive (TP)** ELISA positive Immunosensor positive	**False positive (FP)** ELISA negative Immunosensor positive
Test	–	**False negative (FN)** ELISA positive Immunosensor negative	**True negative (TN)** ELISA negative Immunosensor negative

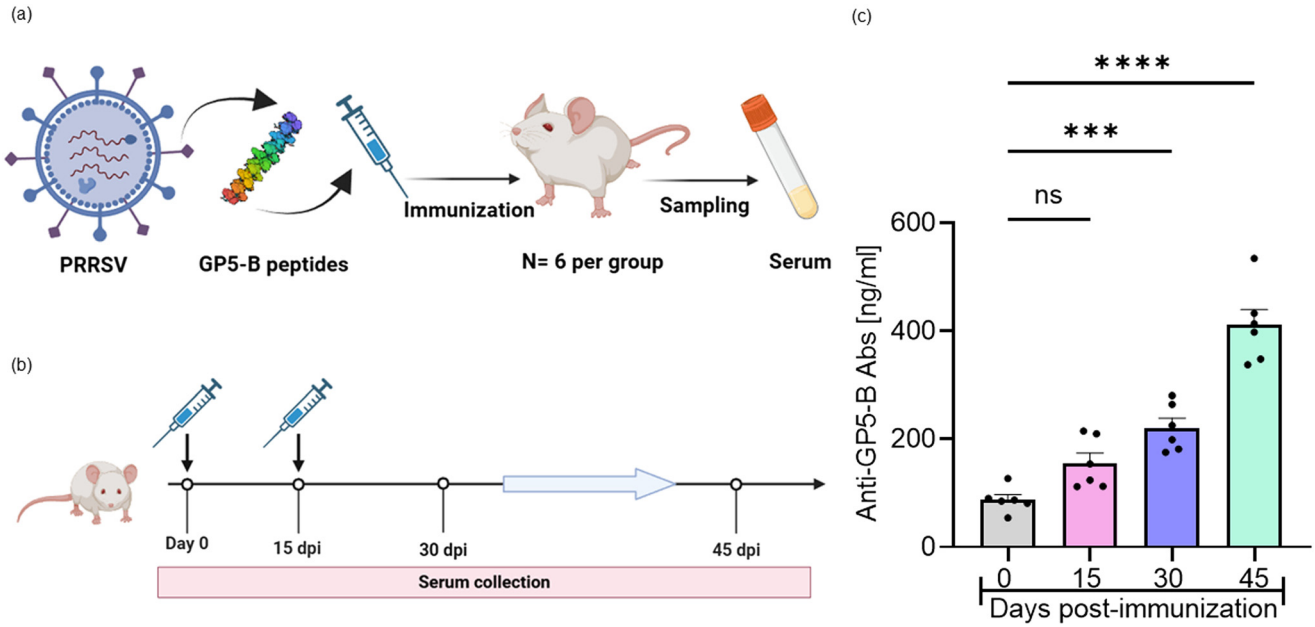

Fig. 1 ELISA quantification of anti-GP5-B antibody responses in a 45 day mouse immunization model. (a) Schematic representation of the immunization strategy. Mice (n = 6) were immunized with GP5-B peptide conjugated to bovine serum albumin (BSA) *via* a maleimide linkage. Serum samples were collected longitudinally following immunization. (b) Immunization timeline. Mice received a primary immunization (day 0) consisting of GP5-B–BSA emulsified in Freund's complete adjuvant, followed by a booster dose (day 15) in Freund's incomplete adjuvant. Blood samples were collected at 0, 15, 30, and 45 days post-immunization (dpi). Control groups included untreated mice and vehicle controls (BSA plus adjuvant only). (c) Quantification of anti-GP5-B IgG antibodies by indirect ELISA. GP5-B peptide was covalently immobilized onto 96-well plates, and antibody concentrations were calculated using a standard curve (0–1000 ng mL^{-1}). Data are presented as mean ± SEM. Statistical significance was evaluated by one-way ANOVA followed by Tukey's *post hoc* test (ns: not significant; ***$p < 0.001$; and ****$p < 0.0001$).

with BSA conjugated with GP5-B *via* a maleimide linkage (GP5-B–BSA), using Freund's complete adjuvant for the prime dose (day 0) and Freund's incomplete adjuvant for the booster dose (15 dpi) (Fig. 1a and b, respectively). Serum samples were collected at days 0, 15, 30, and 45 dpi. Antibody titers were quantified using ELISAs. GP5-B (10 μg mL^{-1}) was covalently immobilized in 96-well plates using a Takara peptide-coating kit, and each serum sample (1 μL) was added to a different well with 99 μL dilution buffer. An IgG standard curve (0–1000 ng mL^{-1}) with purified recombinant IgG (Sigma-Aldrich I4506) and anti-human IgG-HRP secondary antibody (GeneScript A01854) were used to convert absorbance values to antibody concentrations. Day 0 sera and sera from BSA/adjuvant-only control mice served as baselines. This design follows where small viral peptides are conjugated to carrier proteins (*e.g.*, BSA) to induce a strong antibody response.

As shown in Fig. 1c, the mice immunized with GP5-B showed an increase in antibody response. At 15 dpi, the peptide-specific IgG level rose markedly above the baseline (0 dpi) and remained high at 30 and 45 dpi. In contrast, the control mice only maintained a background-level signal throughout. Statistical analysis confirmed that at 15, 30, and 45 dpi, IgG concentrations were significantly higher than preimmune levels ($p < 0.01$–0.0001), indicating that GP5-B elicits a strong humoral immune response. ELISA data reveal that GP5-B immunization produces high-titer, peptide-specific antibodies by 15–45 dpi, whereas preimmune and adjuvant-only sera antibody levels did not change (the data are not shown), suggesting the suitability of GP5-B as a recognized element for antibody detection.

As a result, the generation and validation of specific anti-GP5B antibodies in the murine model provided a controlled set of serum samples with known serological profiles. These characterized sera were subsequently used as analytical inputs to evaluate the performance of the peptide-based electrochemical immunosensor. Thus, the immunized mouse sera served as a reference to assessing the capability of the functionalized biosensor to detect specific antibodies under controlled conditions, prior to its application to swine samples.

GP5-B was used in the EIS-based immunosensor for detecting antigen-specific antibodies. The quantitative behaviors of the immunosensors were evaluated by measuring the charge-transfer resistances (R_{ct}) of different concentrations of anti-GP5-B antibodies. For the immunosensor preparation, AuSPE electrodes were sequentially modified with a TGA self-assembled monolayer, activated with NHS/EDC chemistry, and functionalized with GP5-B peptide, and finally unspecific binding with casein was avoided. Casein was selected after preliminary optimization experiments, comparing with BSA or ovalbumin proteins.

Impedance spectra were generated for the surface-modified electrodes and are presented as Nyquist plots in Fig. 2a. For the AuSPE electrode, the R_{ct} value is 62 Ω. Then,

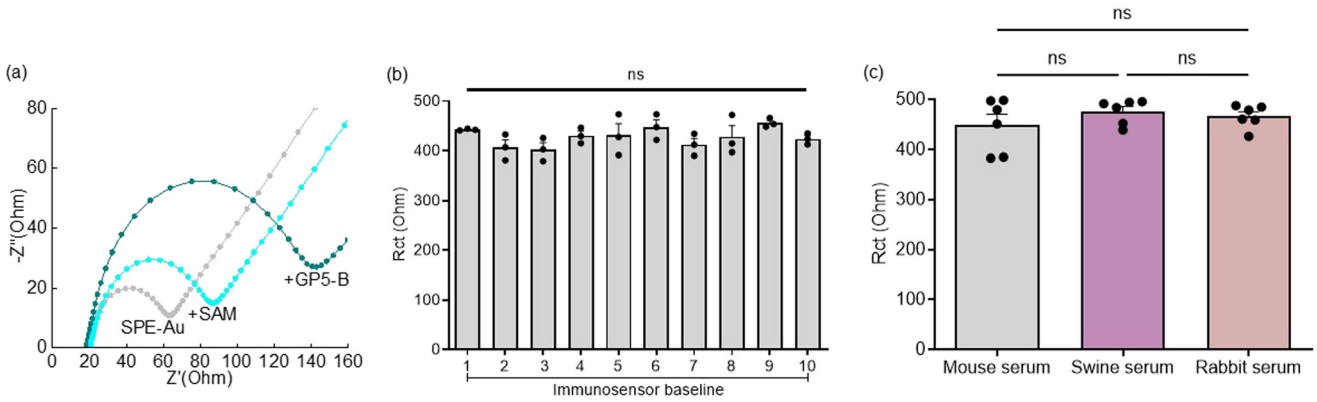

Fig. 2 Fabrication, reproducibility, and specificity characterization of the impedimetric immunosensor. (a) Stepwise electrochemical impedance spectroscopy (EIS) characterization of immunosensor fabrication: (gray) bare screen-printed gold electrode (AuSPE), (cyan) AuSPE functionalized with a thioglycolic acid (TGA) self-assembled monolayer activated with NHS/EDC chemistry, and (turquoise) covalent immobilization of the GP5-B peptide. Nyquist plots show a progressive increase in charge-transfer resistance (R_{ct}) confirming successful surface modification. (b) Reproducibility and stability assessment after blocking non-specific bonds. EIS measurements were performed under analyte-free baseline conditions (5 mM $[Fe(CN)_6]^{3-/4-}$ in PBS, pH 7.2) using 30 independent electrodes (3 technical replicates per electrode) across 10 fabrication batches. No significant differences were observed among batches (one-way ANOVA, $p < 0.05$). The intra-assay and inter-assay coefficients of variation were 5.05% and 4.08%, respectively. (c) Specificity assessment. EIS responses obtained with non-specific sera (non-immunized mice, swine, and rabbit sera; $n = 6$), remained at baseline levels, indicating minimal non-specific binding. Impedance spectra were acquired from 10 mHz to 100 kHz (10 mV AC amplitude) and fitted using a Randles equivalent circuit model (R_s, solution resistance, R_{ct}; charge-transfer resistance; C_{dl}: double-layer capacitance, and W; Warburg impedance). Data are presented as mean ± SEM.

the SAM (R_{ct} = 90 Ω) formed by the addition of TGA was attached to the AuSPE electrode, and GP5-B (R_{ct} = 150 Ω) was immobilized on the activated electrode surface (TGA-NHS/EDC), increasing R_{ct}.

The modified electrodes were incubated with casein, which further increased the charge-transfer resistance (R_{ct}) to approximately 400 Ω. Consistent electrochemical responses were observed across 30 independently prepared electrodes. For repeatability assessment, ten independent batches were prepared, each consisting of three immunosensors. Measurements were performed in triplicate for each electrode. The intra-assay coefficient of variation (CV) was 5.05%, and the inter-assay CV was 4.08% (Fig. 2b); the data showed non-significant differences among batches. Sera from non-immunized mice, non-vaccinated pigs, and rabbits were used to compare the complexity of the blood serum. These samples showed impedance responses comparable to baseline values (Fig. 2c). In this case, the intra-assay CV was 7.31% and the inter-assay CV was 2.97%, supporting the analytical assessment.

The modified electrodes (TGA-NHS/EDC) were further incubated with 1 μL serum from a GP5-B-immunized mouse before calibration with the blank sample, and R_{ct} increased (ΔR_{ct} = 600 Ω). Fig. 3a shows the Nyquist plots for the modified electrodes incubated with different serum antibody concentrations, with a linear range from 0 to 42 ng mL^{-1}

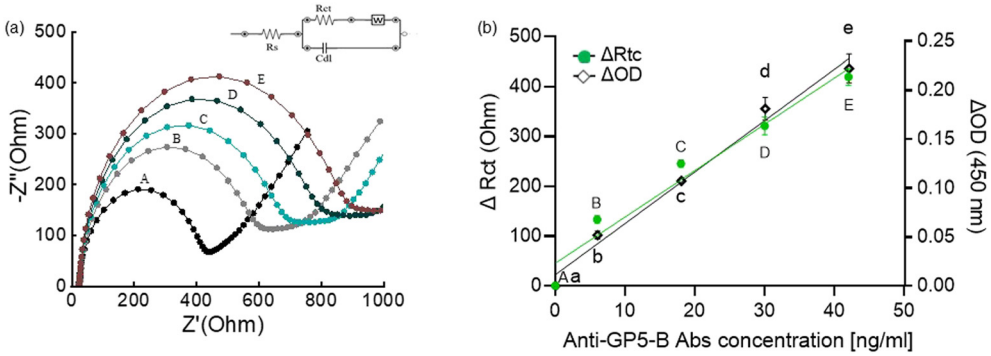

Fig. 3 Analytical performance of the impedimetric immunosensor and correlation with ELISA measurements. (a) Representative Nyquist plots showing EIS responses to increasing concentrations of anti-GP5-B antibodies: (A, black) 0 ng mL^{-1}(baseline), (B, gray) 6 ng mL^{-1}, (C, cyan) 18 ng mL^{-1}, (D, turquoise) 30 ng mL^{-1}, and (E, red) 42 ng mL^{-1}. Measurements were conducted in 5 mM $[Fe(CN)_6]^{3-/4-}$ over a frequency range of 10 mHz to 100 kHz (10 mV amplitude; n = 3 technical replicates). Data were fitted using the Randles equivalent circuit. (b) Comparative analytical correlation between the immunosensor and ELISA. The linear relationship between ΔR_{ct} (R_{ct}, sample − R_{ct}, baseline R^2 = 0.9541) and ELISA absorbance change at 450 nm (ΔOD_{450nm}; R^2 = 0.9636) demonstrates strong agreement between both analytical platforms within the 0–42 ng mL^{-1} antibody concentration range, supporting the reliability of the proposed immunosensor for quantitative anti-PRRSV antibody detection.

after serum addition from GP5-B-immunized mice, while Fig. 3b shows the linear regression of the antibody concentration *vs.* ΔR_{ct} relationship, revealing a correlation coefficient of R^2 = 0.9541, and compares the plots of the antibody concentration *vs.* ΔR_{ct} relationship obtained using both the immunosensors and ELISA (ΔOD_{450nm}; R^2 = 0.9636). Compared to the baseline EIS signal (R_{ct} = 400 Ω at a serum antibody concentration of 0 ng mL^{-1}), the EIS signal intensified to R_{ct} = 600, 700, 850, and 900 Ω with increasing serum antibody concentration to 6, 18, 30, and 42 ng mL^{-1}, respectively.

Based on Fig. 3, the lowest antibody concentration evaluated was 0.6 ng mL^{-1}, which produced a reproducible and clearly impedimetric signal relative to the baseline. At this concentration, an approximate increase of 200 Ω in R_{ct} was observed compared with the blank measurement, exceeding baseline variability confirming reliable signal discrimination. Therefore, the LOD of the proposed immunosensor was established at 6 ng mL^{-1}, corresponding to the lowest concentration tested and consistent with the statistical 3σ criterion.[24]

The immunosensor's responses to antibodies in the GP5-B-immunized mice were compared with the responses to the control mice (*e.g.*, the intact-animal control and maleimide-carrier/BSA-immunized groups). The results showed statistically significant differences between the GP5-B-immunized and both the control and BSA-immunized groups (Fig. 4a–d).

The immunosensor's responses to antibodies in the naturally infected and vaccinated swine were compared with the responses to the control swine (PRDC free and nonvaccinated animals). The results showed statistically significant between-group differences (Fig. 5a–e).

These results demonstrate that the GP5-B functionalized impedimetric immunosensor is capable of selectively and sensitively discriminating between sera containing GP5-B specific antibodies and control sera lacking antigen-specific immune responses. The significantly higher R_{ct} values observed in GP5-B immunized mice, compared with the controls, confirm that the measured impedimetric charges arise from specific antigen–antibody interactions at the electrode surface. This clear separation between experimental and control groups validates the GP5-B peptide as an effective recognition element. Importantly, the robust and reproducible detection of peptide-specific antibodies in a controlled murine model provides strong experimental support for the proposed diagnostic applications, establishing a reliable proof of concept prior to translation to vaccinated and naturally infected swine samples.

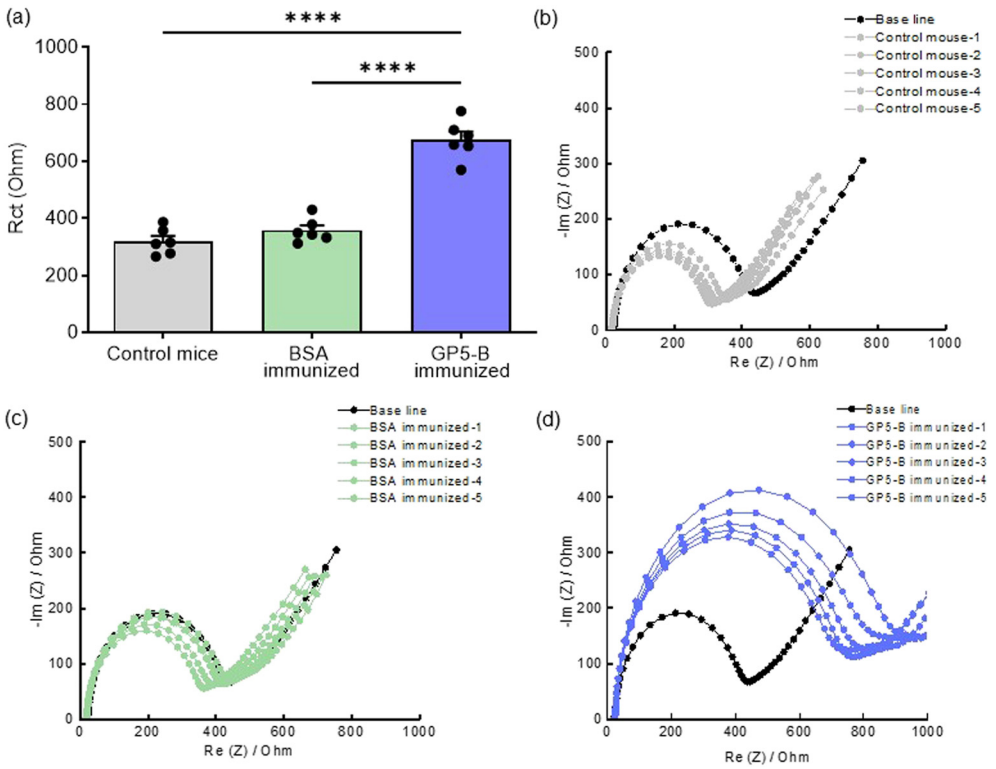

Fig. 4 Detection of anti-GP5-B antibodies in the mouse serum using the impedimetric immunosensor. (a) Charge-transfer resistance (R_{ct}, Ω) values obtained from preimmune sera, BSA-immunized controls, and GP5-B-immunized mice. Data represent n = 6 mice per group with n = 3 technical replicates per sample. (b and c) Representative Nyquist plots for control sera (non-immunized mice) and GP5-B-immunized mice, respectively. (d) Comparative analysis demonstrating significantly higher R_{ct} values in GP5-B-immunized mice compared with preimmunized mice and BSA control groups. Impedance spectra were recorded from 10 mHz to 100 kHz (10 mV amplitude) and modeled using the Randles equivalent circuit. Data are expressed as mean ± SEM. Statistical significance was determined by one-way ANOVA followed by Tukey's *post hoc* test (****$p <$ 0.0001).

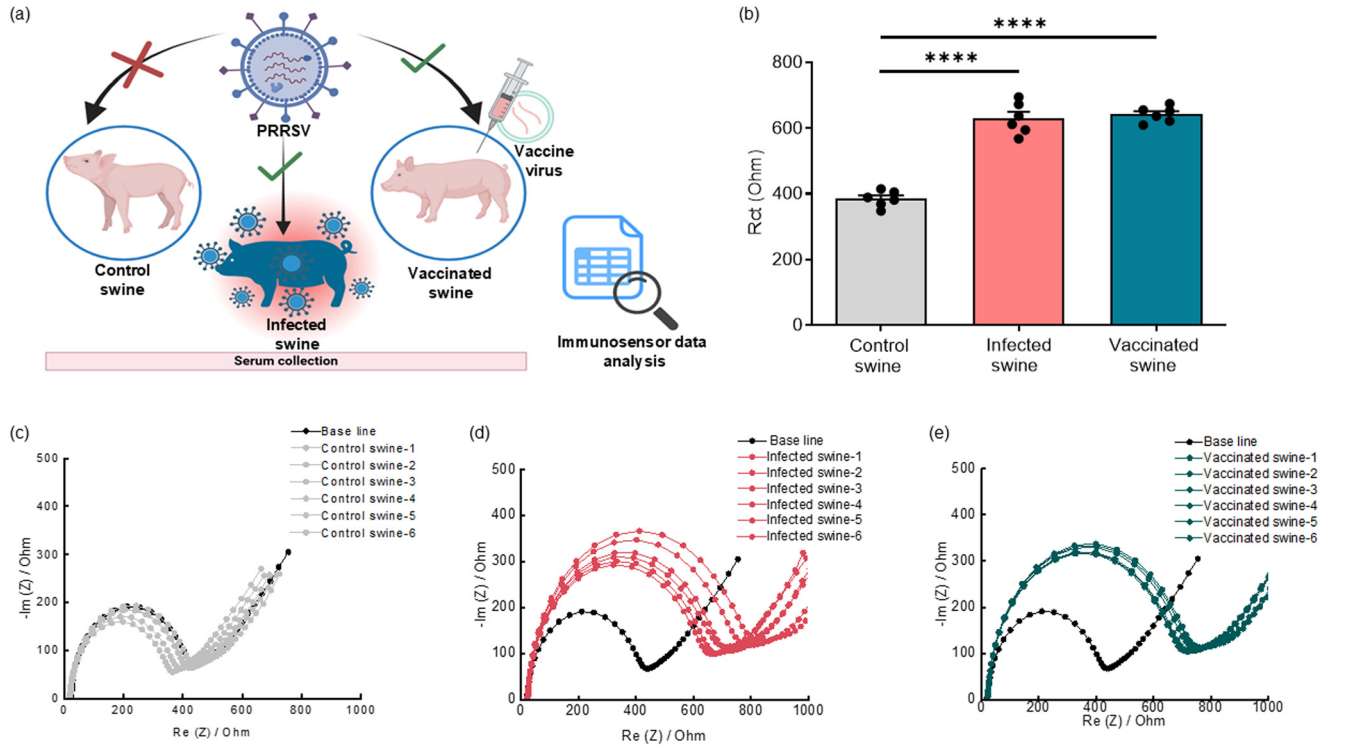

Fig. 5 Detection of anti-PRRSV antibodies in porcine serum using the peptide-based impedimetric immunosensor. (a) Experimental workflow schematic. Serum samples were collected from three groups: PRRSV-negative controls, naturally infected pigs, and pigs vaccinated with a modified live virus (MLV) PRRSV vaccine. Samples were analyzed using the GP5-B peptide-functionalized impedimetric immunosensor. (b) Summary of immunosensor responses. Bar graphs showing the change in charge-transfer resistance (ΔR_{ct}) for each group (means ± SEM, n = 6 pigs per group). ΔR_{ct} represents the increase in R_{ct} relative to blank measurements. Infected and vaccinated animals showed significantly higher ΔR_{ct} values compared with controls (****$p < 0.0001$). (c–e) Representative Nyquist plots corresponding to the control, infected, and vaccinated pig sera. Measurements were performed in 5 mM ferri/ferrocyanide ($[Fe(CN)_6]^{3-}/^{4-}$, 1 : 1) over a frequency range of 0.1 Hz to 100 kHz (10 mV amplitude). Increased semicircle diameters indicate higher charge-transfer resistance due to antibody binding. Data were fitted using a Randles equivalent circuit model.

To determine whether the test result was positive or negative, the cutoff point was analyzed using an ROC curve plotting R_{ct}-derived sensitivity and specificity percentages for the control and experimental groups (n = 54), representing 100% for each group. For each possible cutoff point, the tabulated values between positive and negative test results are shown ($p < 0.0001$). A 95% confidence interval was obtained. The biosensor exhibited 100% sensitivity and 93.33% specificity, making it suitable for detecting antibodies (Fig. 6) and confirming the feasibility of practically applying the proposed GP5-B-probe-based immunosensor for detecting anti-PRRSV antibodies.

Overall, these results demonstrate that the proposed immunosensor effectively discriminates between PRRSV-seropositive and seronegative swine under biologically relevant conditions. The significantly higher ΔR_{ct} values observed in both naturally infected and vaccinated pigs, compared with PRDC-free and nonvaccinated controls, indicate that the biosensor reliably detects circulating anti-PRRSV antibodies generated by either natural infection or immunization. The consistent impedimetric responses across these clinically relevant groups highlight the robustness of the GP5-B peptide as a recognition element and underscore

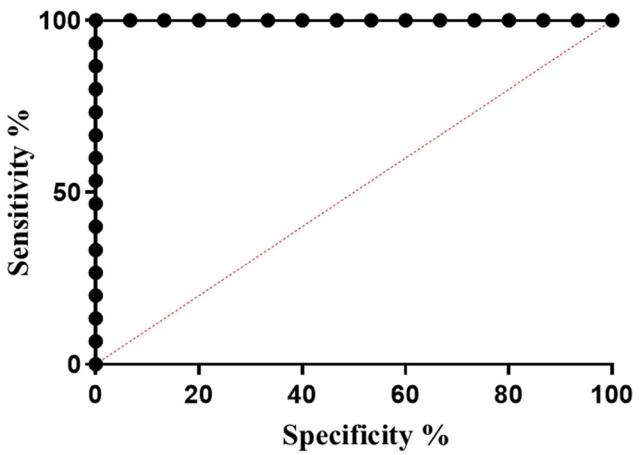

Fig. 6 Receiver operating characteristic (ROC) curve evaluating the diagnostic performance of the immunosensor assay. The ROC curve illustrates the relationship between sensitivity and specificity derived from control and experimental groups across different cutoff thresholds. The area under the curve (AUC) indicates strong diagnostic performance ($p < 0.0001$; 95% confidence interval reported). The immunosensor achieved 100% sensitivity and 93.3% specificity for anti-PRRSV antibody detection.

the diagnostic potential of the proposed platform for serological surveillance and herd-level monitoring of PRRSV exposure.

Conclusions

(i) Gold-coated screen-printed electrodes demonstrated robust analytical performance, supporting their suitability for antibody detection platforms.

(ii) AuSPEs only required small samples, were less expensive than other conventional antibody detection methods, and provided immediate results.

(iii) The immunosensor calibration revealed analyte-dependent linearity and yielded an LOD of 6 ng mL^{-1}.

(iv) The immunosensor selectively detected anti-PRRSV antibodies, without any interference from other proteins, compared with other animal species serum proteins.

(v) The biosensor exhibited 100% sensitivity and 93.3% specificity.

The proposed biosensor was applied to detect specific antibodies in a mouse model and pigs in farms, and this could represent a useful tool for detecting PRRSV antibodies and contributing to biosecurity and animal health.

Concluding remarks

Because they are more stable than other biosensor probes, peptide-based recognition elements enable the improvement of sensing processes. Because peptides comprise short chains of amino acids, they are chemically more stable than proteins. In addition, because of their unique characteristics, peptides enable the industrial-scale manufacture of biosensors and maintain their stability long term.[25]

Usually, peptide-based electrochemical biosensors integrate a specific peptide sequence as the main component, modified with a thiol for peptide immobilization. However, although immunosensors can be developed using peptide antigens or antibody biorecognition elements, they can also integrate antibody or antigen fractions.

Immunosensors are based on specific antigen–antibody interactions and can be a tool for quantitatively or qualitatively detecting antigen-specific antibodies.[26]

Although the preliminary results are promising, extensive field validation studies are required to confirm diagnostic performance across diverse epidemiological conditions. Likewise, the stability of the immunosensor over time could be evaluated for future research.

The proposed GP5-derived peptide immunosensor represents a promising alternative for rapid PRRSV antibody detection, combining analytical sensitivity, specificity, and operational simplicity, which may facilitate on-site serological surveillance in swine production systems.

Author contributions

Conceptualization, methodology, and writing – original draft: L. E. F. C., R. E. N. A., L. A. O. F., G. E. and A. B. P.; data curation and formal analysis: L. E. F. C., F. P.-D., F. C. R., M. L. J. G., D. D. H. and A. G. Z. A.; investigation: L. E. F. C., F. P. D., F. C. R., A. G. Z. A. and R. C. V.; resources and supervision: R. E. N. A., L. A. O. F. and A. B. P.; writing – review & editing: R. E. N. A., L. E. F. C. and L. A. O. F.; visualization: L. E. F. C. and R. E. N. A.; funding acquisition: R. E. N. A., L. A. O. F. and A. B. P.

Conflicts of interest

The authors declare that they have no conflict of interest regarding this study.

Data availability

All data are incorporated into the article, without supplementary information (SI). The data will be shared upon reasonable request to the corresponding author.

Acknowledgements

We thank the Project CONACYT CB A1-S-43236 for the partial funding. We are also grateful to grants CONACYT INFR-255010 and 317189. We are grateful to the partial funding by the CIC-UMSNH funding (2023–2025). We are grateful to the CIDETEQ-CONACYT for the facilities to develop the project. We thank the fellowship 732727 L. E. F. C. CONACYT.

References

1 N. Music and C. A. Gagnon, *Anim. Health Res. Rev.*, 2010, **11**, 135–163.
2 S. M. López-Heydeck, R. A. Alonso-Morales, H. Mendieta-Zerón and J. C. Vázquez-Chagoyán, *Rev. Mex. Cienc. Pecu.*, 2015, **6**, 69–89.
3 C. S. Kristensen, M. G. Christiansen, K. Pedersen and L. E. Larsen, *Porcine Health Manag.*, 2020, **6**, 26.
4 Z. Zhang, Z. Li, H. Li, S. Yang, F. Ren, T. Bian, L. Sun, B. Zhou, L. Zhou and X. Qu, *Front. Vet. Sci.*, 2022, **9**, 1024720.
5 T. Dokland, *Virus Res.*, 2010, **154**, 86–97.
6 S. Montaner-Tarbes, H. A. Del Portillo, M. Montoya and L. Fraile, *Front. Vet. Sci.*, 2019, **6**, 38.
7 F. Perez-Duran, F. Calderon-Rico, L. E. Franco-Correa, A. G. Zamora-Aviles, R. Ortega-Flores, D. Durand-Herrera, A. Bravo-Patino, R. Cortes-Vieyra, I. Hernandez-Morales and R. E. Nunez-Anita, *Vaccines*, 2024, **12**, DOI: 10.3390/v16010014.
8 Q. Luo, Y. Zheng, H. Zhang, Z. Yang, H. Sha, W. Kong, M. Zhao and N. Wang, *Animals*, 2023, **13**, DOI: 10.3390/ani13050813.
9 C. Montagnese, P. Barattini, A. Giusti, G. Balka, U. Bruno, I. Bossis, A. Gelasakis, M. Bonasso, P. Philmis, L. Denes, S. Peransi, M. Rodrigo, S. Simon, A. Griol, G. Wozniakowski, K. Podgorska, C. Pugliese, L. Nannucci, S. D'Auria and A. Varriale, *Sensors*, 2019, **19**, DOI: 10.3390/s19020407.
10 X. Tian, H. Wang, Z. Liu, Z. Wei, Y. Yang, H. Wang, G. Liu, H. Song, X. Huang and T. An, *Front. Cell. Infect. Microbiol.*, 2025, **15**, 1616898.

11 O. Hosu, G. Selvolini, C. Cristea and G. Marrazza, *Curr. Med. Chem.*, 2018, **25**, 4119–4137.
12 F. Yang, Y. Li, X. Jin, Q. Xu, F. Cheng and X. Wang, *J. Appl. Microbiol.*, 2020, **129**, 1751–1757.
13 J. Zhao, L. Zhang, J. Cao, Y. Yu, B. Ma, Y. Jiang, J. Han and W. Wang, *Anal. Chem.*, 2024, **96**, 11092–11102.
14 P. Norouzi, M. Nezamoddini and M. R. Safarnejad, *Int. J. Environ. Anal. Chem.*, 2023, **103**, 546–560.
15 U. Jarocka, R. Sawicka, A. Gora-Sochacka, A. Sirko, W. Zagorski-Ostoja, J. Radecki and H. Radecka, *Biosens. Bioelectron.*, 2014, **55**, 301–306.
16 E. Mikula, C. E. Silva, E. Kopera, K. Zdanowski, J. Radecki and H. Radecka, *BMC Vet. Res.*, 2018, **14**, 328.
17 S. Klangprapan, C. C. Weng, W. T. Huang, Y. K. Li and K. Choowongkomon, *ACS Omega*, 2021, **6**, 24233–24243.
18 F. Li, R. Zhou, K. Zhao, H. Chen and Y. Hu, *Talanta*, 2011, **87**, 302–306.
19 L. Yuan and L. Liu, *Sens. Actuators, B*, 2021, **344**, 130232.
20 Y. Yu, L. Zhang, B. Wang, J. Zhao, K. Han, Y. Qi, J. Li, X. Wang, B. Sun, J. Zhang, J. Cao, B. Ma, X. Peng, J. Cao, Y. Ke and W. Wang, *J. Am. Chem. Soc.*, 2025, **147**, 11049–11061.
21 P. S. Sfragano, G. Moro, F. Polo and I. Palchetti, *Biosensors*, 2021, **11**, 246.
22 X. Li, S. Zhou, Q. Zhao, Y. Chen, P. Qi, Y. Zhang, L. Wang, C. Guo and S. Chen, *Angew. Chem., Int. Ed.*, 2023, **62**, e202216987.
23 R. E. Nunez-Anita, F. Calderon-Rico, F. Perez-Duran, M. C. Arenas-Arrocena, A. G. Zamora-Aviles, L. E. Franco-Correa, A. Bravo-Patino and I. Hernandez-Morales, *Can. J. Vet. Res.*, 2023, **87**, 110–119.
24 International Union of Pure and Applied Chemistry (IUPAC), 5.0.0 edn, 2025, DOI: 10.1351/goldbook.L03540.
25 S. Neethirajan, *Sens. Biosensing Res.*, 2017, **12**, 15–29.
26 A. Karimzadeh, M. Hasanzadeh, N. Shadjou and M. d. l. Guardia, *TrAC, Trends Anal. Chem.*, 2018, **107**, 1–20.